Study of Baryon form factors at BESIII

Xiaorong Zhou

State Key Laboratory of Particle Detection and Electronics
University of Science and Technology of China

Workshop of the Baryon Production at BESIII, Hefei, China
9.15th, 2019

Outline

- Introduction
- Baryon Form factors
  - Nucleon form factors
  - Hyperon form factors
- Summary and prospect

Composition of the Universe

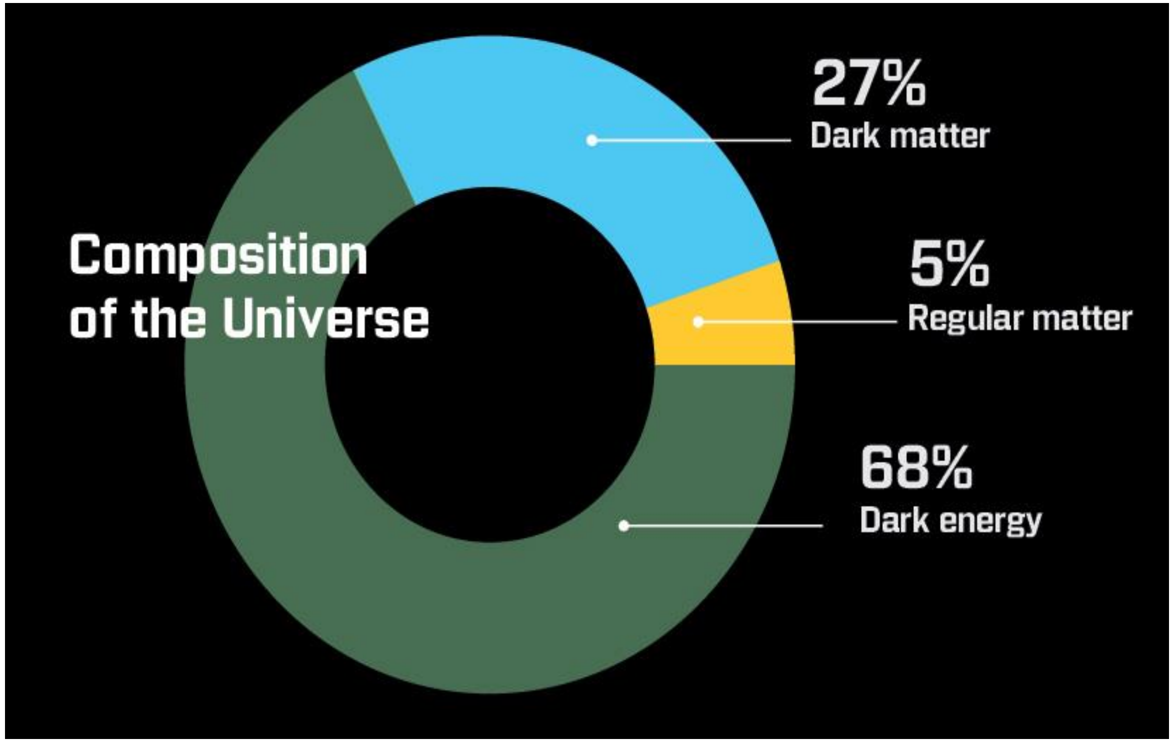

NASA

- Nucleon is the dominant component of visible universe (>99%)

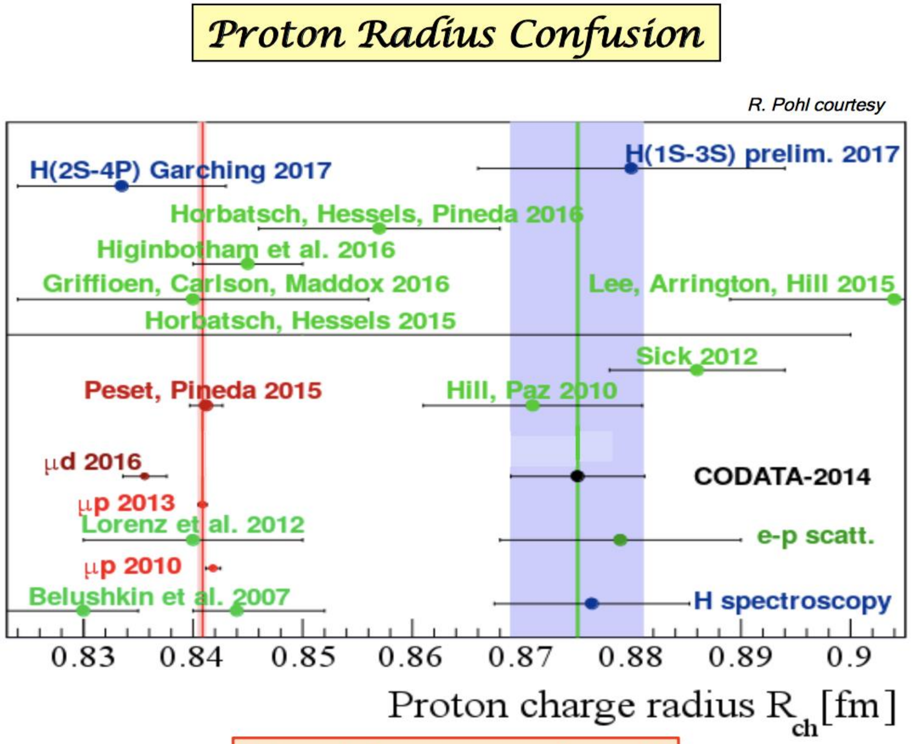

Need for more data !!

- Probe nucleon charge radius:

$$G_E(Q^2) = 1 - \frac{1}{6} r_E^2 Q^2 + \cdots$$ （Q：four momentum transfer）

Nucleon Electromagnetic Form Factor (NEFF)

- Elastic scattering of electron and proton (Hofstadter, Nobel Prize 1961)
  - Theoretically, differential cross section is:

$$\left(\frac{d\sigma}{d\Omega}\right)_{ep}=\left(\frac{d\sigma}{d\Omega}\right)_{Mott}\left(1+2\tau\tan^2\frac{\theta}{2}\right)F(q^2)$$

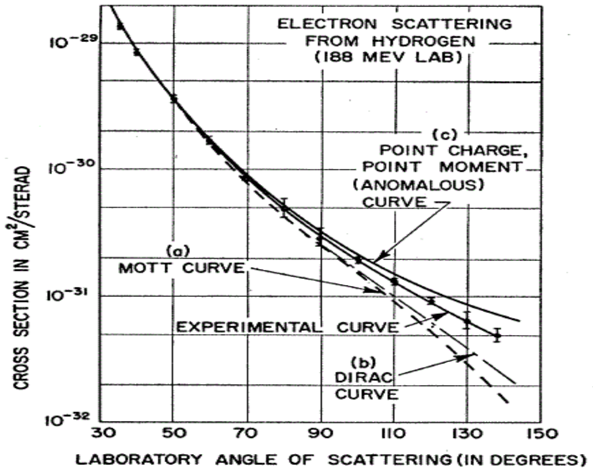

- The nucleon electromagnetic vertex Γ_μ describing the hadron current:

$$\Gamma_\mu(p',p)=\gamma_\mu F_1(q^2)+\frac{i\sigma_{\mu\nu}q^\nu}{2m_p}F_2(q^2)$$

- Sachs FFs:

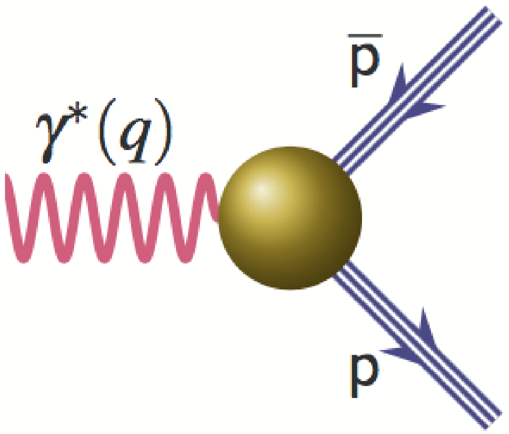

Electric FF： $G_E(q^2)=F_1(q^2)+\tau\kappa_p F_2(q^2)$

Magnetic FF： $G_M(q^2)=F_1(q^2)+\kappa_p F_2(q^2)$

$$\tau=\frac{q^2}{4m^2},\qquad \kappa=\frac{g-2}{2},\qquad g=\frac{\mu}{J}$$

Playground of EMFFs

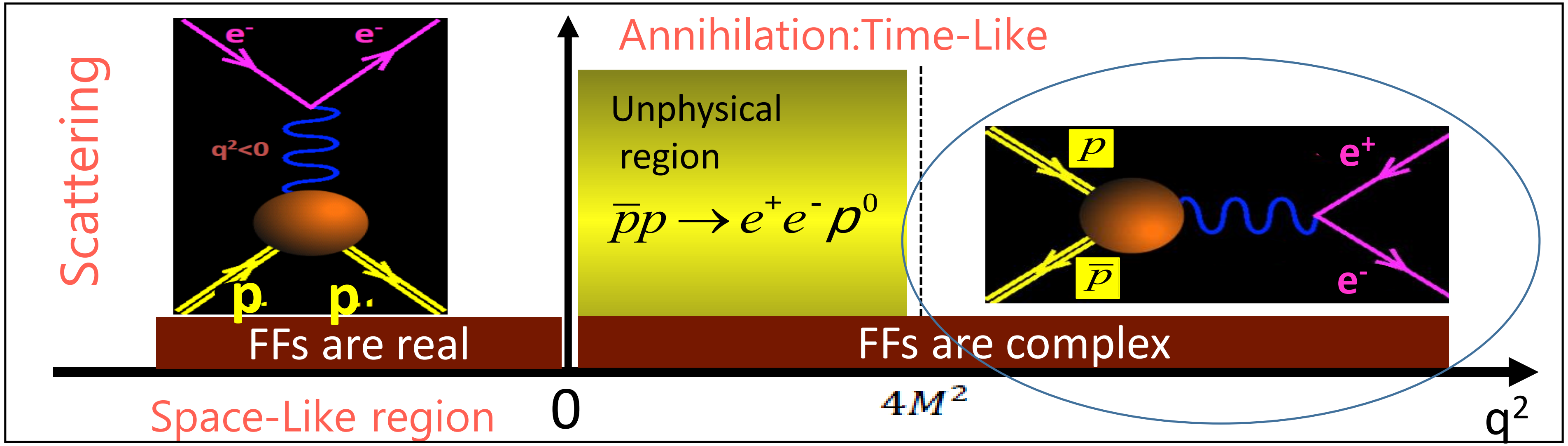

- **In SL**, FFs are real.
  - Encode information about charge distribution of the nucleon
- **In TL**, FFs are complex, $|G_E/G_M|$ and $\Delta\Phi$.
  - Can be related to the time evolution of the EM charges within the nucleon
- BESIII has access to the FFs in TL

Measurement techniques for baryon FF

	Energy Scan	Initial State Radiation
E_{beam}	discrete	fixed
$\mathcal{L}$	low at each beam energy	high at one beam energy
σ	$\frac{d\sigma_{p\bar{p}}}{d(\cos\theta)} = \frac{\pi\alpha^2\beta C}{2q^2}[\lvert G_M\rvert^2(1+\cos^2\theta)$ $+\frac{4m_p^2}{q^2}\lvert G_E\rvert^2\sin^2\theta]$	$\frac{d^2\sigma_{p\bar{p}\gamma}}{dq^2 d\theta_\gamma} = \frac{1}{s}W(s,x,\theta_\gamma)\sigma_{p\bar{p}}(q^2)$ $W(s,x,\theta_\gamma) = \frac{\alpha}{\pi x}(\frac{2-2x+x^2}{\sin^2\theta_\gamma} - \frac{x^2}{2})$
q^2	single at each beam energy	from threshold to s

$\sim \frac{1}{400}$

Both techniques, energy scan and initial state radiation. can be used at BESIII

Status on proton FFs

- Still mystery on proton cross section line-shape

Phys. Rew. D 87, 092005 (2013)

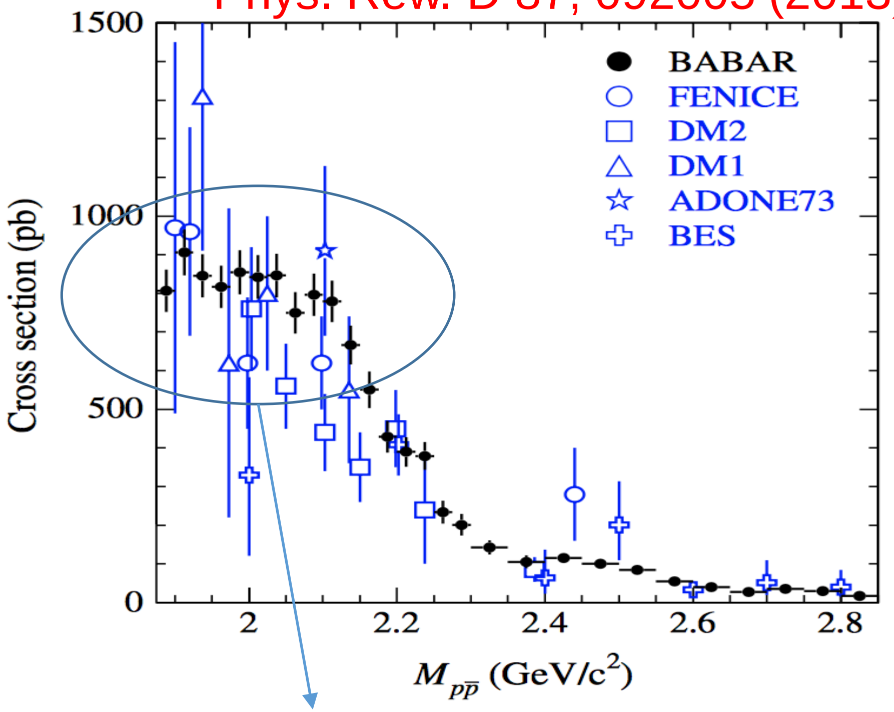

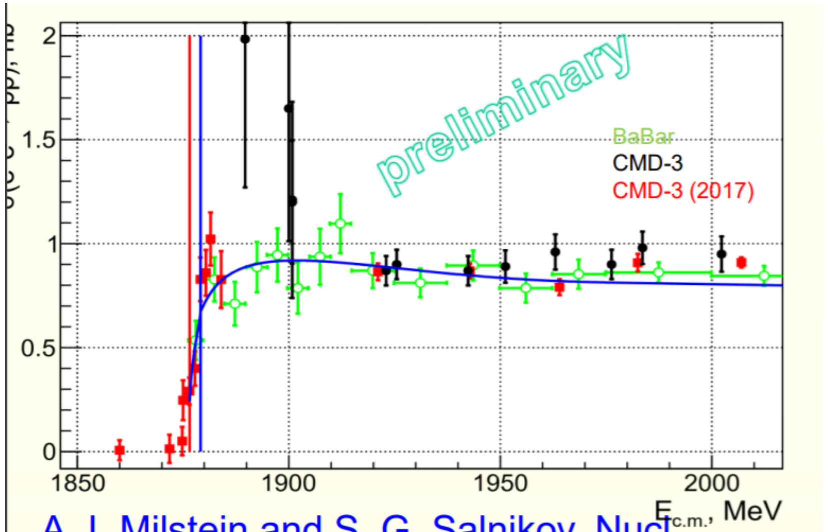

A. I. Milstein and S. G. Salnikov, Nucl. Phys. A 977 , 60 (2018)

- Point-like cross section near threshold,
- $\sigma_{\text{point}} = \frac{\pi\alpha^2}{3m^2\tau}[1 + \frac{1}{2\tau}]$

- The e+e- → ppbar cross section shows an exponential growth in 1 MeV interval above threshold.

Status on proton FFs

- Inconsistence on $|G_E/G_M|$ of proton & poor precision

Phys. Rew. D 87, 092005 (2013)

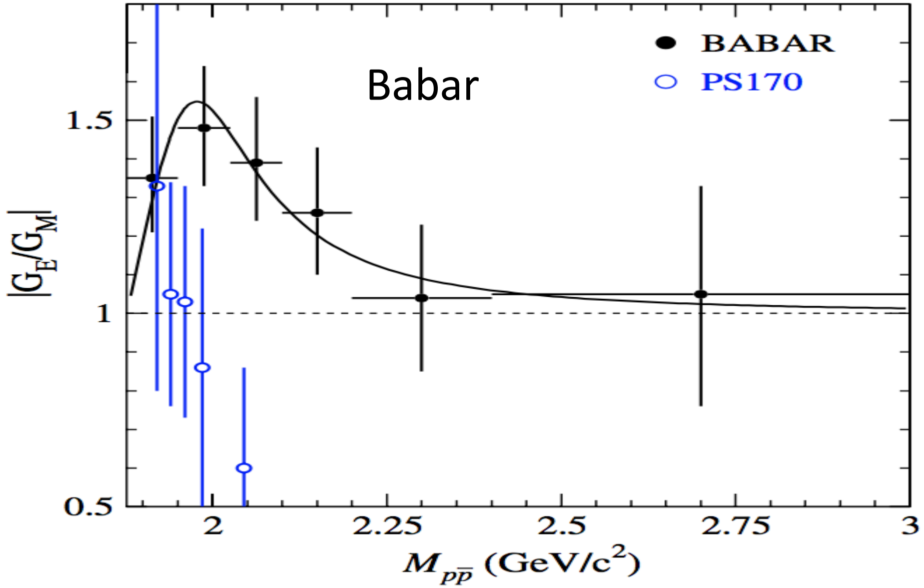

- pQCD predictes a continuous transition and SL-TL equality at high Q^2
- SL best accuracy in $Q^2(0.5, 8.5)$ GeV^2: 1.7%
- TL accuracy before BESIII: exceeding 20%

Status on neutron FFs

- Poor precision, limited q^2 range in neutron FF

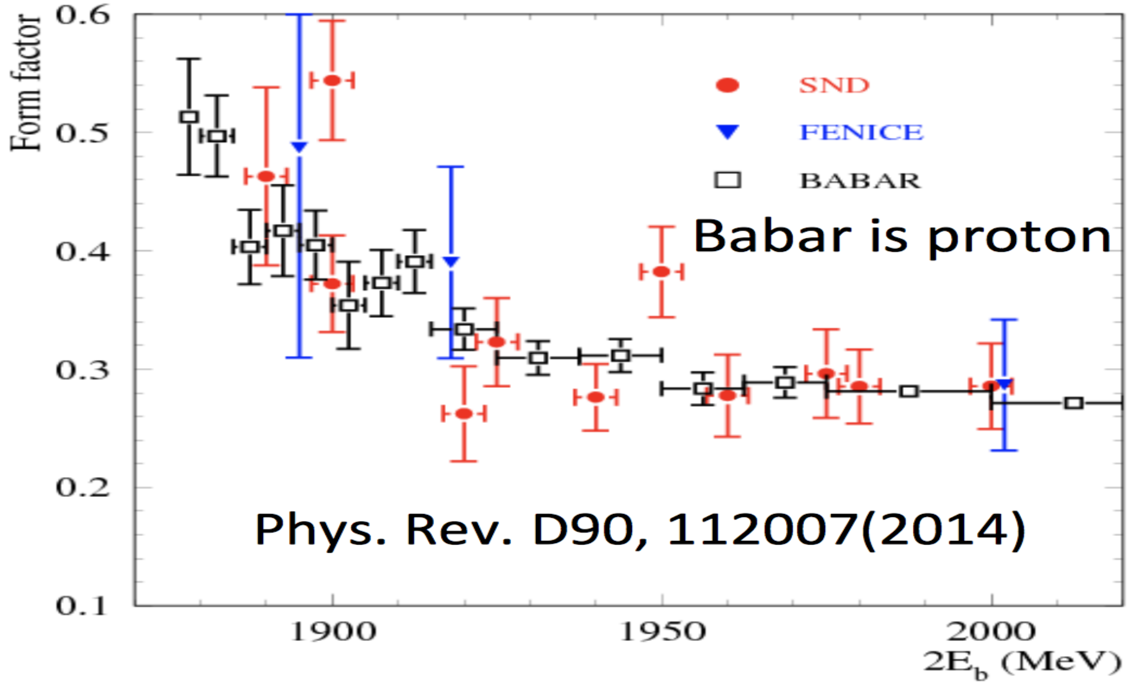

- pQCD prediction[1]: $|\frac{G_M^n}{G_M^p}|^2 \approx (\frac{q_d}{q_u})^2 = 0.25$
- VMD prediction[2]: $|\frac{G_M^n}{G_M^p}|^2 \approx 1$

[1] V. L. Chernyak and I. R. Zhitnitsky, Nucl. Phys. B 246 (1984) 52.
[2] J. G. Körner and m. Kuroda, Phys. Rev. D 16 (1988) 2165.

BESIII data samples

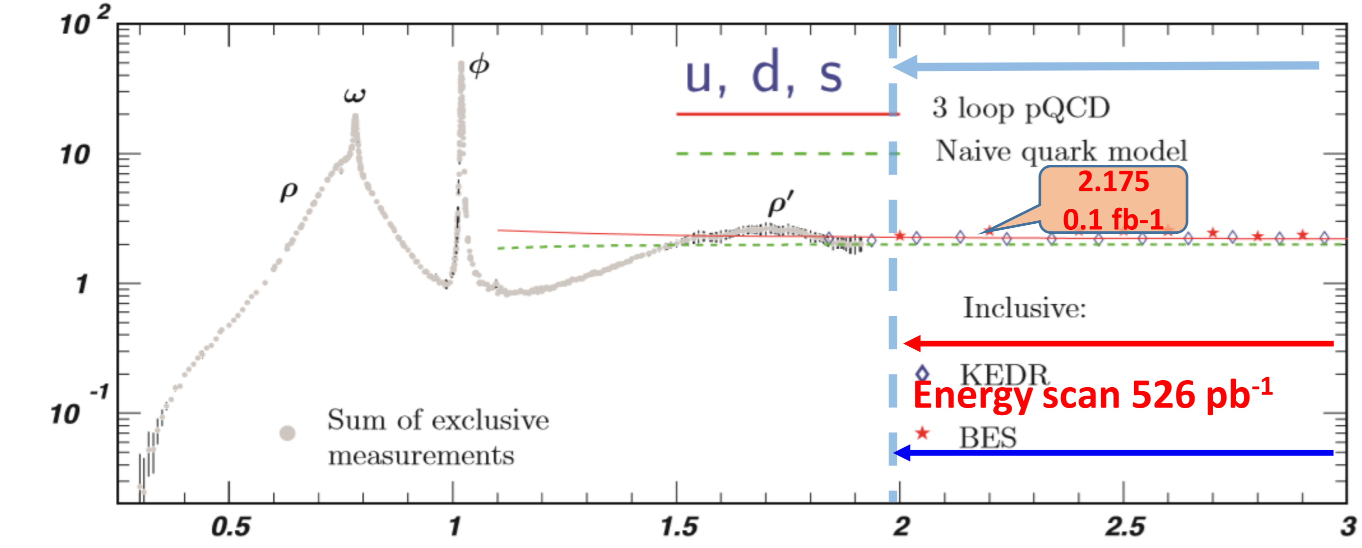

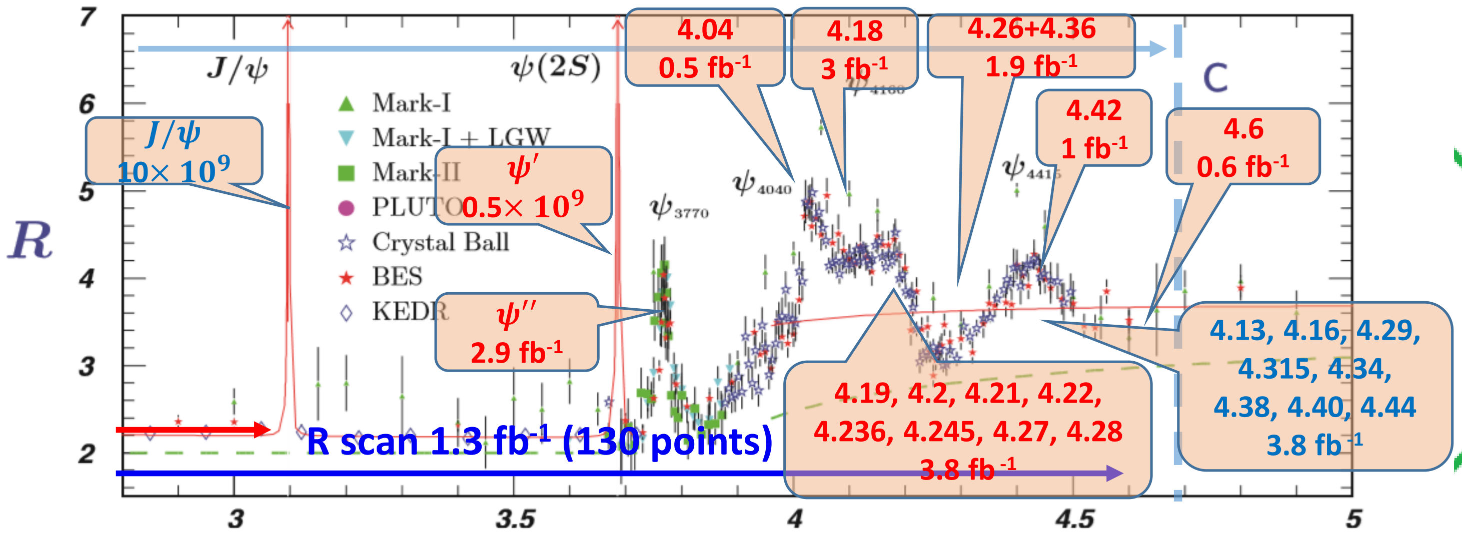

Scan technique

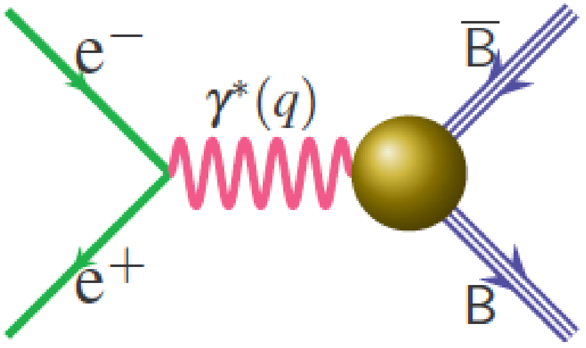

ISR technique

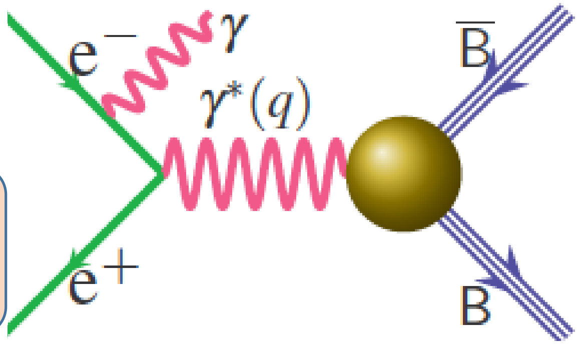

Proton FFs with ISR technique

Phys. Rev. D99, 092002 (2019)

- Combined seven data samples (7.4 fb^{-1})

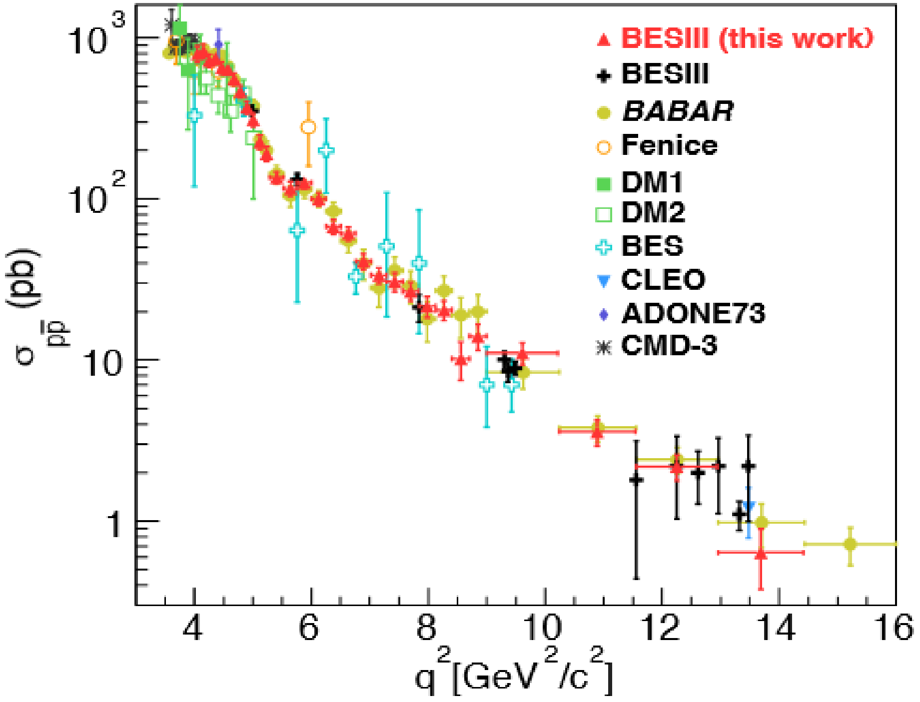

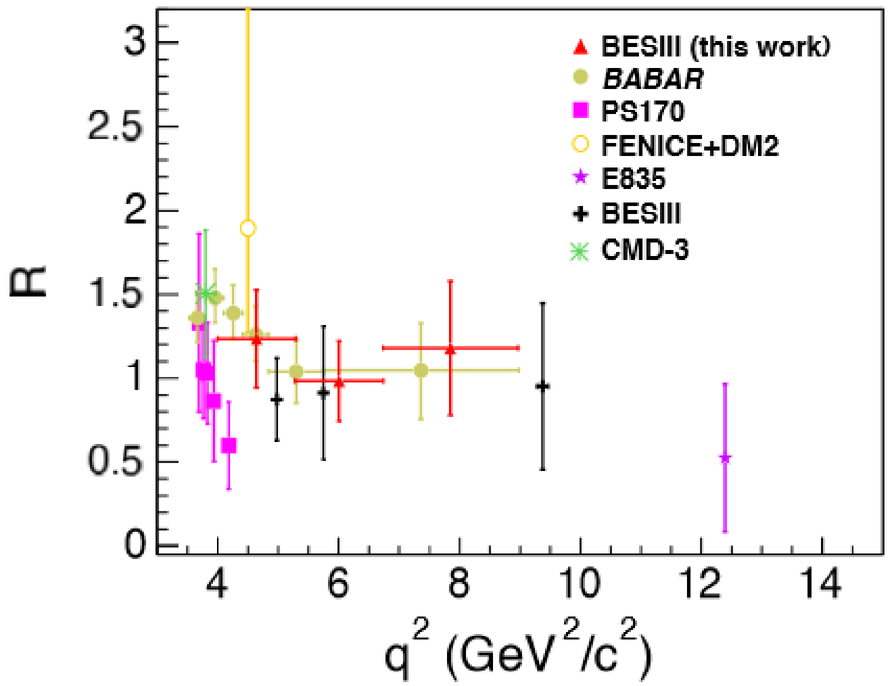

- Precision on $|G_{eff}|$: 4.1%-28.7%(untagged)
- Precision $|G_E/G_M|$ ratio: 23.0%-31.4%(untagged)
- Confirm Babar's result on $|G_E/G_M|$ above threshold

Proton FFs with scan technique

arxiv:1905.09001

- Precise measurement of cross section $e^+e^- \to p\bar{p}$ at 22 points from 2.0 to 3.08 GeV, 688.5 pb^{-1}
- $|G_E/G_M|$, $|G_M|$ are determined with high accuracy, with uncertainty comparable to data in SL
- $|G_E|$ is measured for the first time

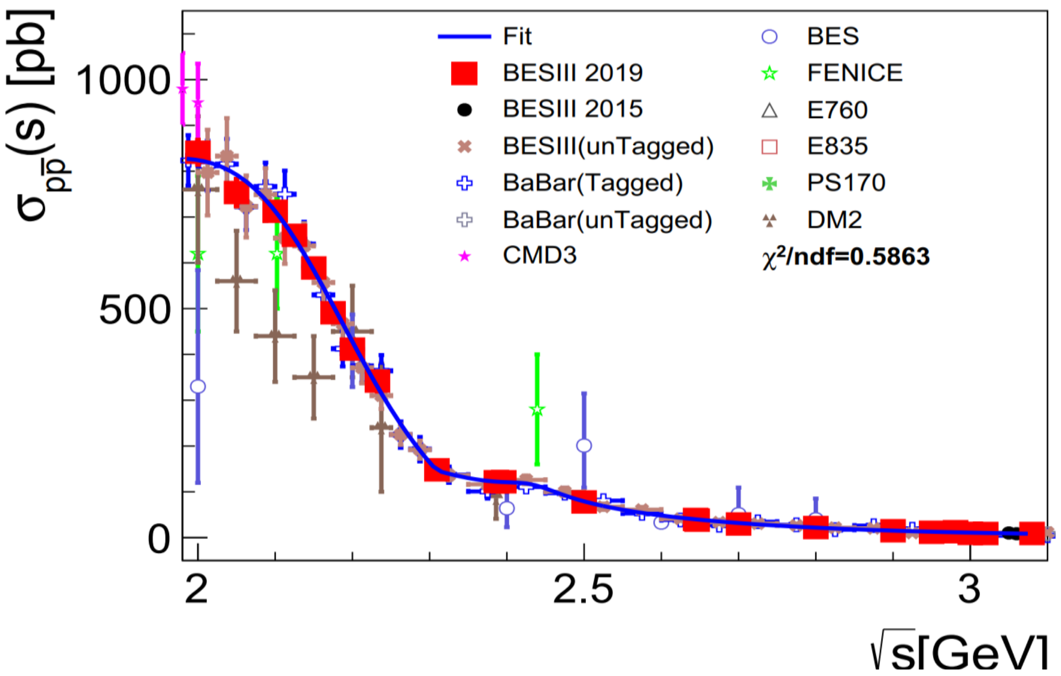

Best precision on σ: 3% (systematic dominant)

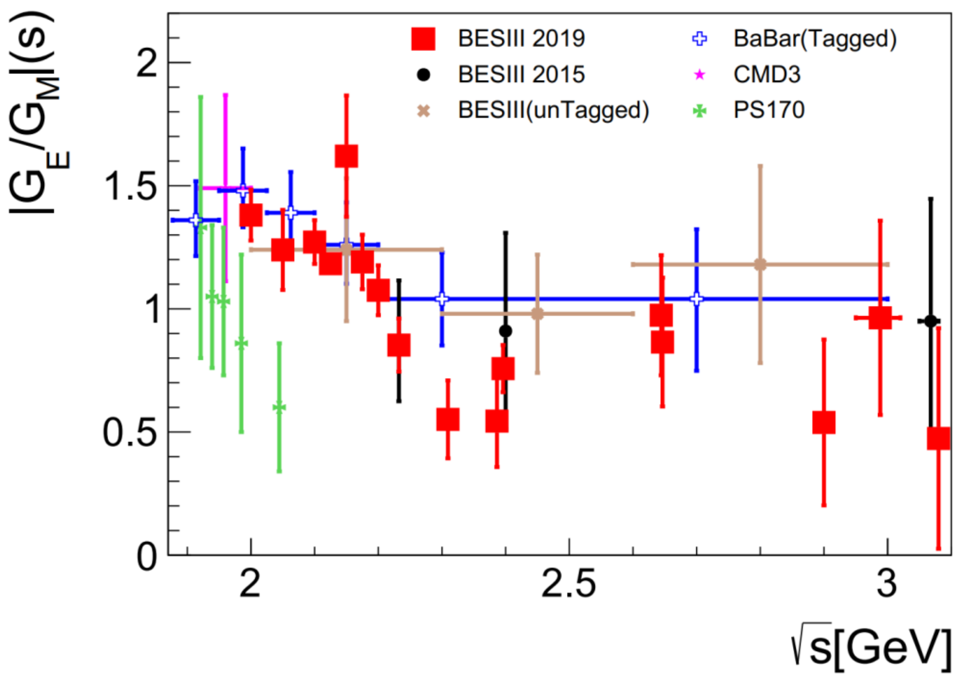

Best precision on $|G_E/G_M|$: 3.4% (statistical dominant)

Proton FFs with scan technique

arxiv:1905.09001

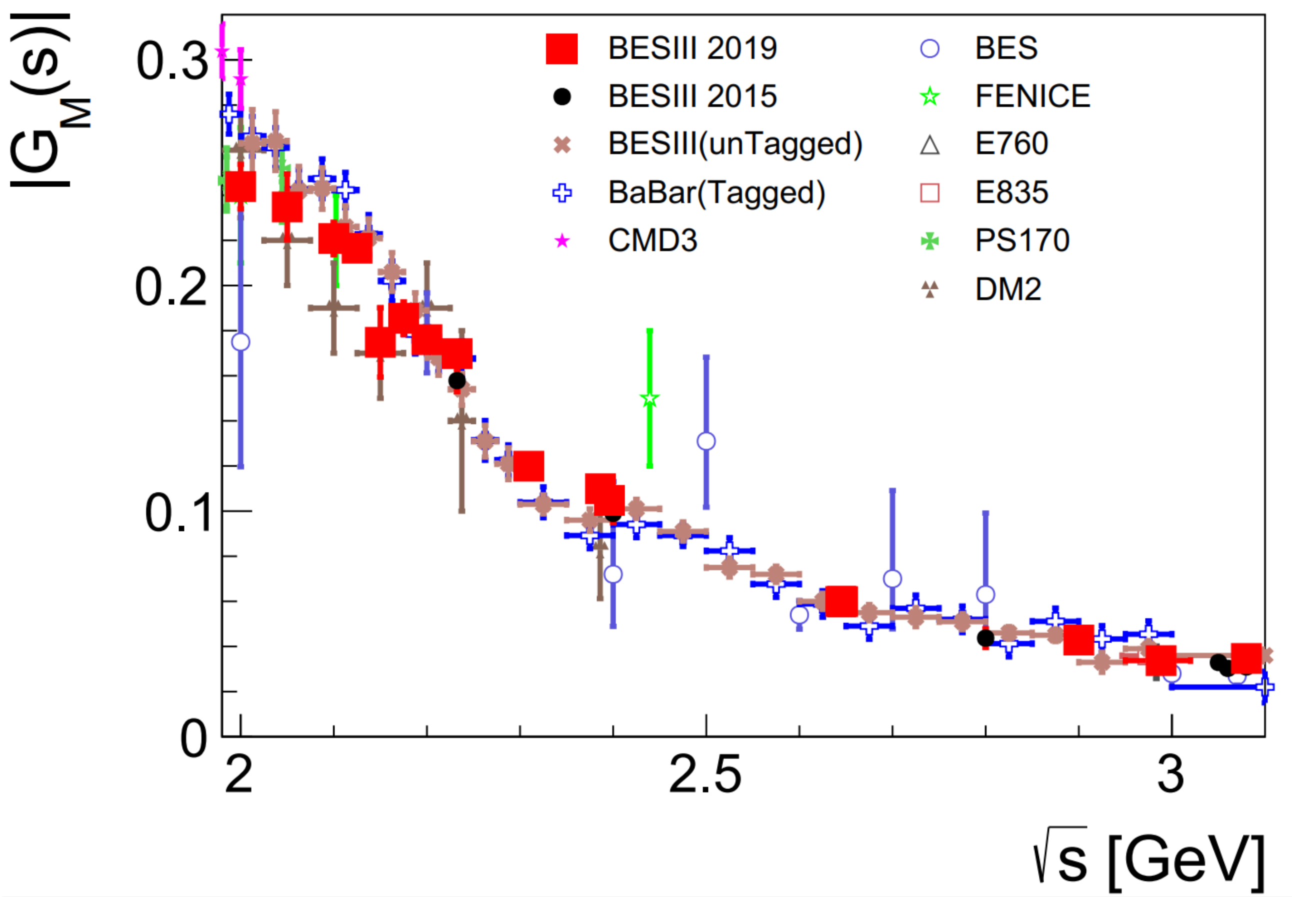

- Hypothesis on other results: $|G_E|=|G_M|$
- First line-shape of $|G_M|$ without hypothesis, achieved by BESIII scan data.

Oscillation structures ?

PRL. 114, 232301 (2015)

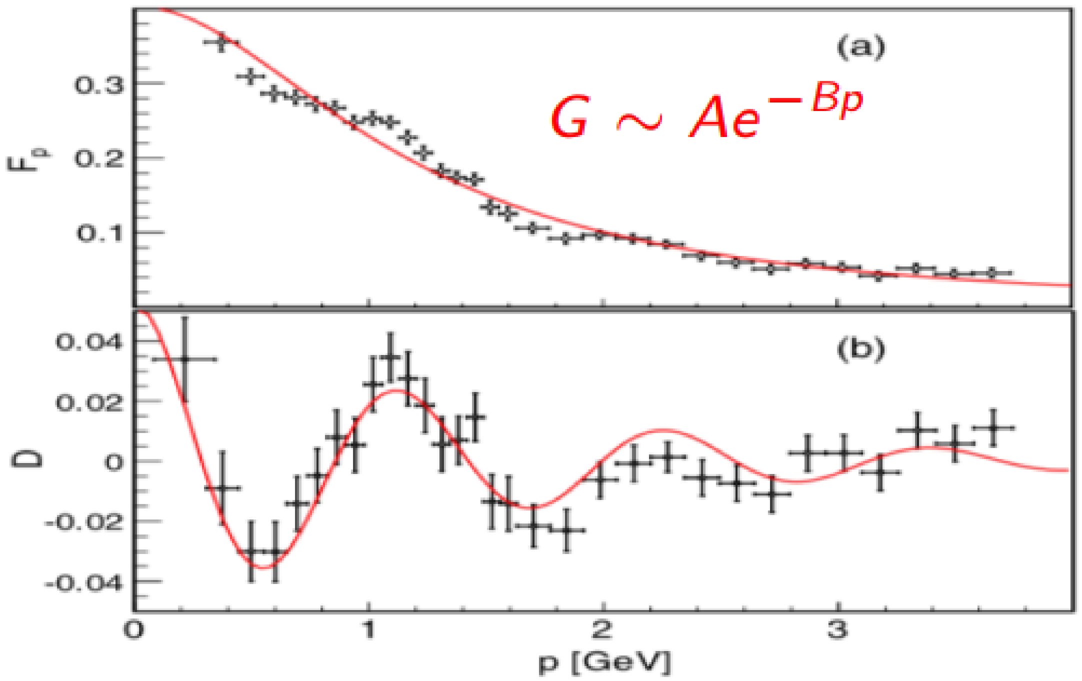

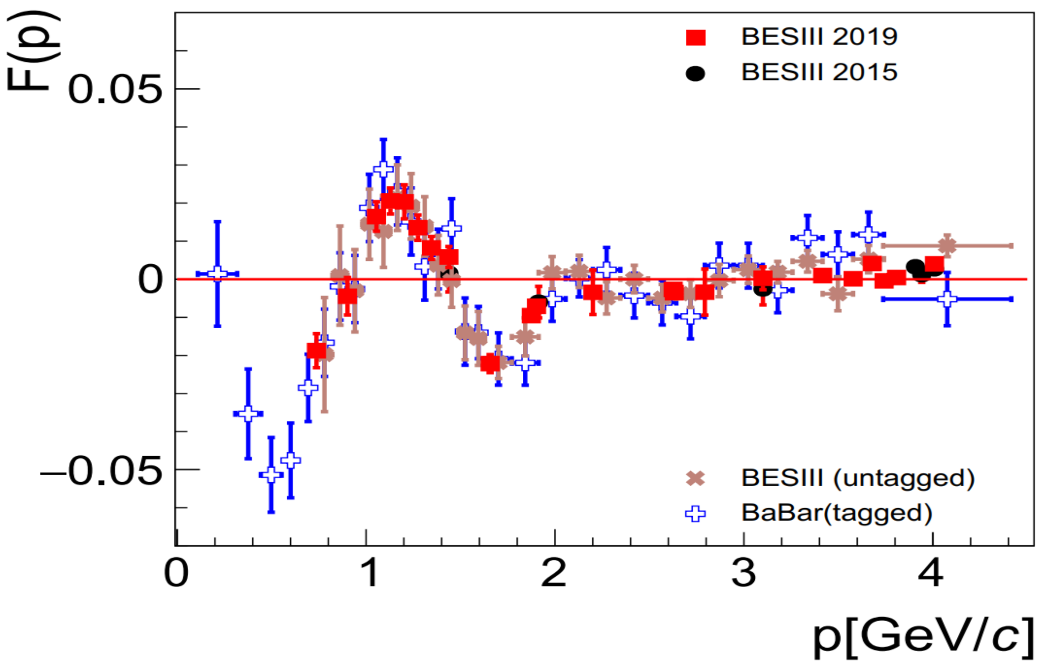

- Oscillating structures observed in the EFF minus modified dipole parameterization in Babar.
  - Rescattering process in final state
  - Independent resonant structure

Neutron form factors at BESIII

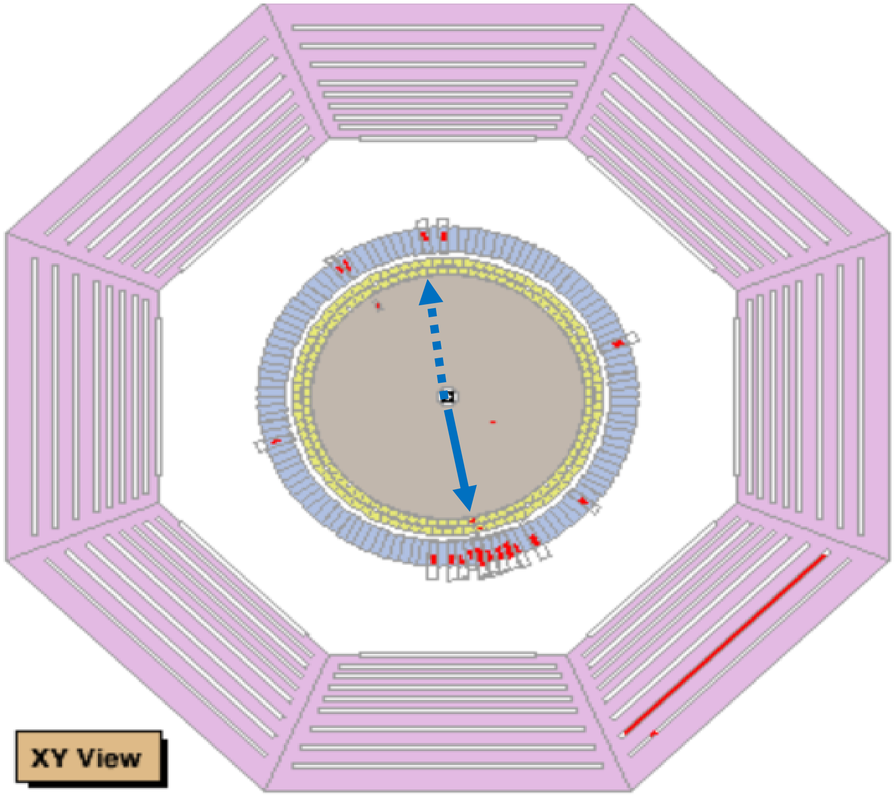

- Analysis Challenges: Reconstruction of $e^+e^- \to n\bar{n}$
  - No MDC signal
  - Low EMC efficiency,
  - No TOF reconstruction

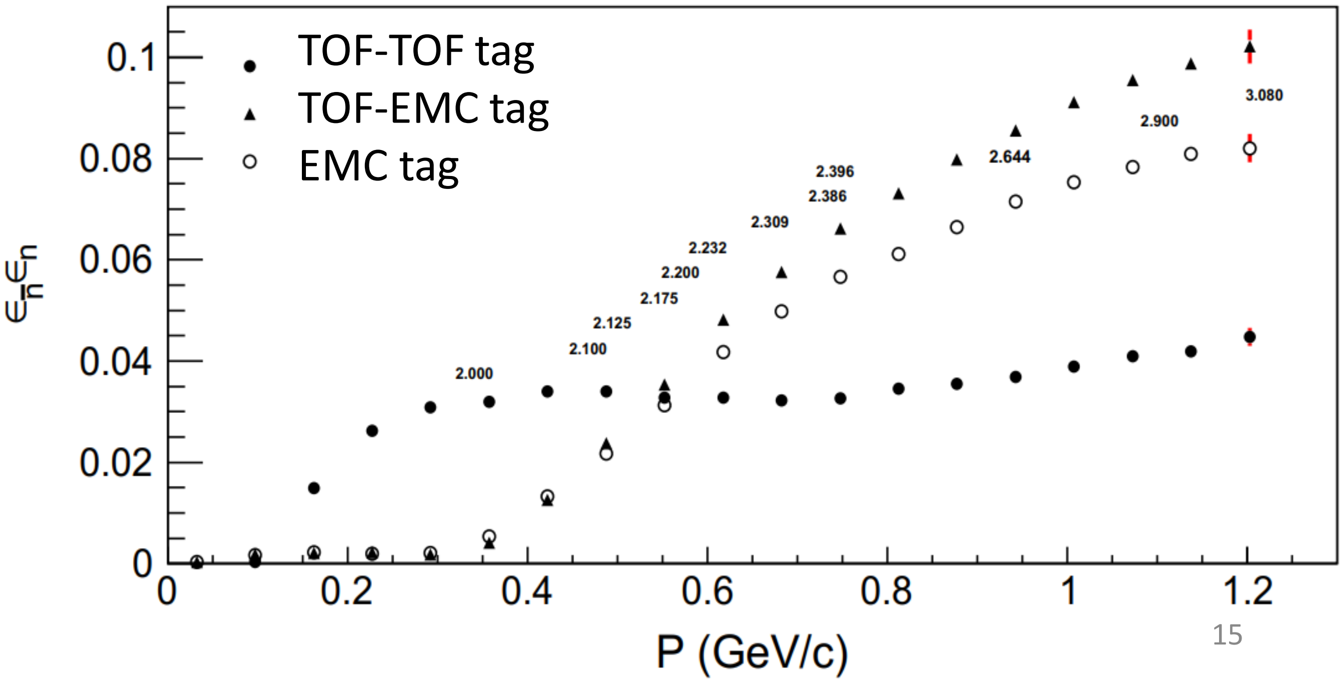

Neutron form factors at BESIII

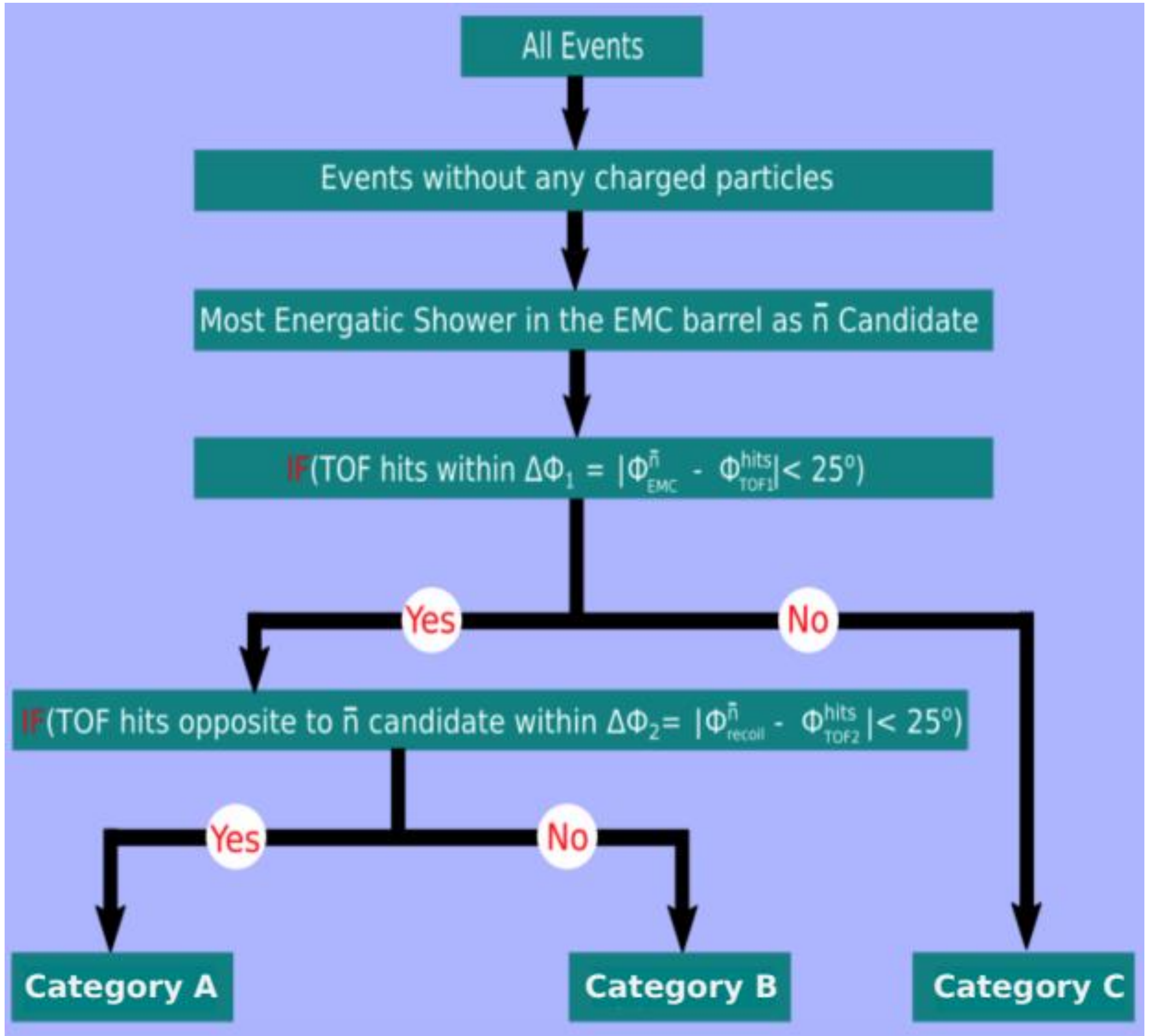

- **Event must be selected by only one of the three categories.**

- **Events in each of the three categories undergo a complete independent analysis:**
  - ✓ Selection Criteria
  - ✓ Signal yield extraction
  - ✓ Efficiency determination
  - ✓ Corrections for efficiency
  - ✓ Cross section determination

Comparison with Space-Like Results

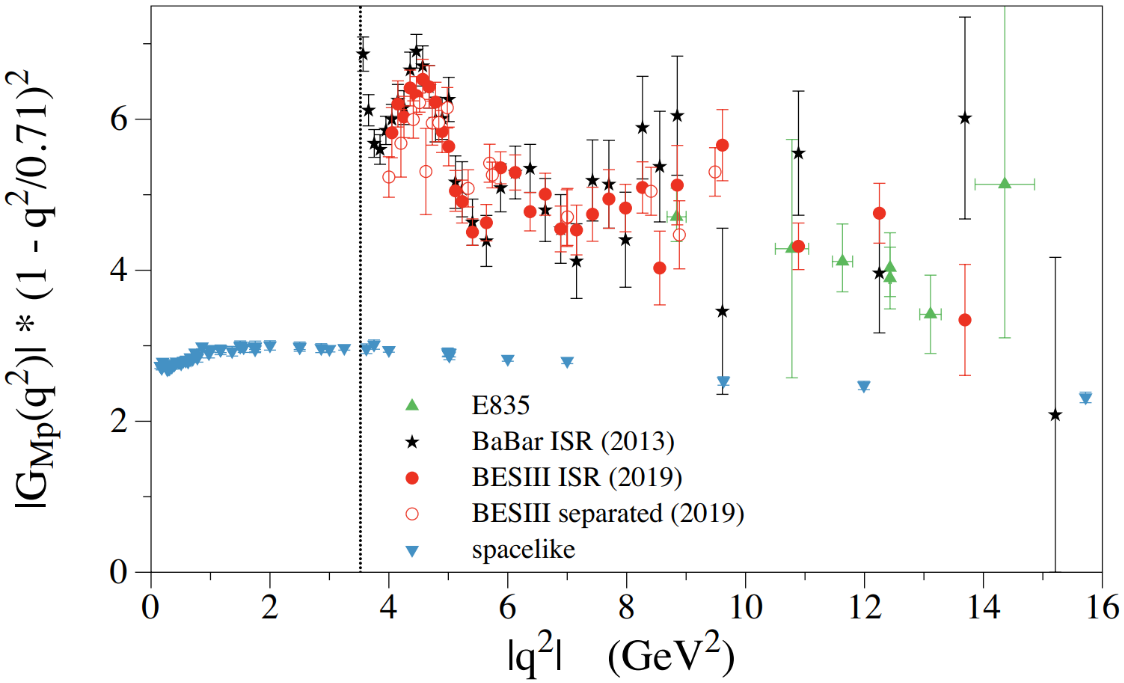

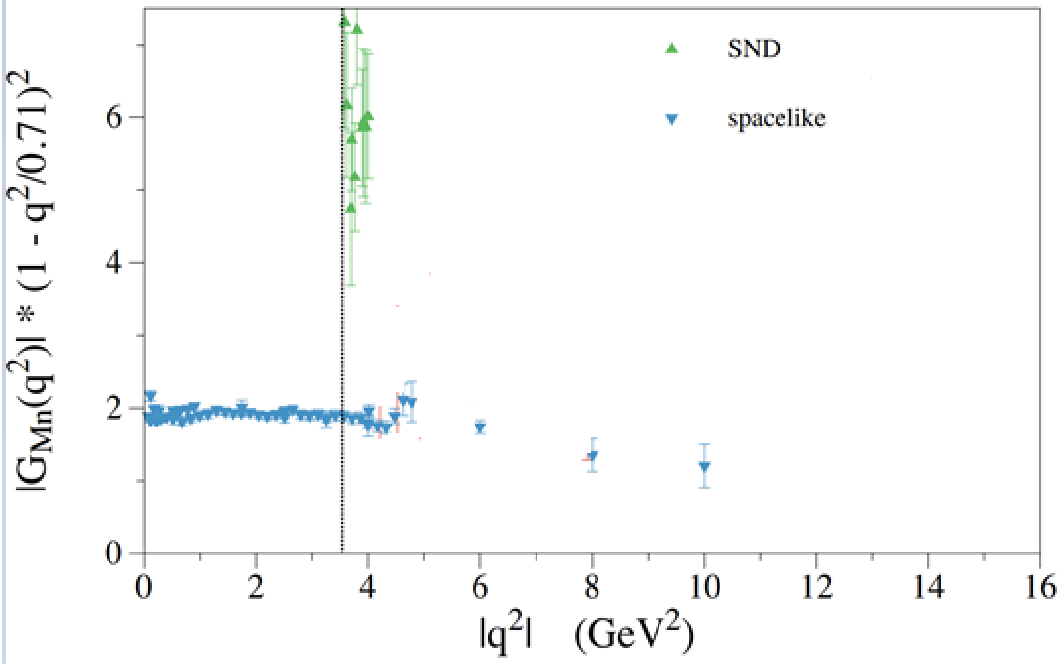

- Neutron and Proton Magnetic Form Factors in the SL and TL regions:
  - The pQCD predicts an asymptotic behavior of the form factors in the SL and TL regions.
  - At high q^2, the pQCD predicts $G_M(SL)=G_M(TL)$ for neutron and proton form factors.
  - The neutron and proton form factors in the TL region are larger than those in the SL region.

Angular Analysis for the Extraction of R_{EM} and $|G_M|$ FFs

The R_{EM} and $|G_M|$ form factors can be extracted by fitting the efficiency corrected angular distribution:

$$\frac{d\sigma^{Born}_{n\bar{n}}}{dcos\theta_{\bar{n}}} = \frac{d\mathcal{N}/dcos\theta_{\bar{n}}}{\epsilon^{MC}_{n\bar{n}} \times \mathcal{C}_{dm} \times \mathcal{C}_{trg} \times (1+\delta) \times \mathcal{L}_{Int}} = A \times |G_M|^2 \left[(1 + cos^2\theta_{\bar{n}}) + R^2_{em}\frac{4M^2_n}{s}(1 - cos^2\theta_{\bar{n}})\right]$$

- $R^2_{em} = |G_E/G_M|$ is the form factor ratio, $A = \frac{2\pi\alpha^2\beta}{4s}$ is the normalisation factor.

Integration over bin width of the fit function is performed due to the large bin width:

$$\left(\frac{d\sigma^{Born}_{n\bar{n}}}{dcos\theta_{\bar{n}}}\right)_i = \sum_{bin=1}^{bin=n}\int_{bin} A_i \times |G_M|^2 \left[(1 + cos^2\theta_{\bar{n}}) + R^2_{em}\frac{4M^2_n}{s}(1 - cos^2\theta_{\bar{n}})\right]$$

- i stands for the three categories, i.e A, B and C.

The neutron form factors are extracted by performing a simultaneous fit to the angular distributions from the three categories where the R_{EM} is shared.

Results of Magnetic Form Factor of the Neutron

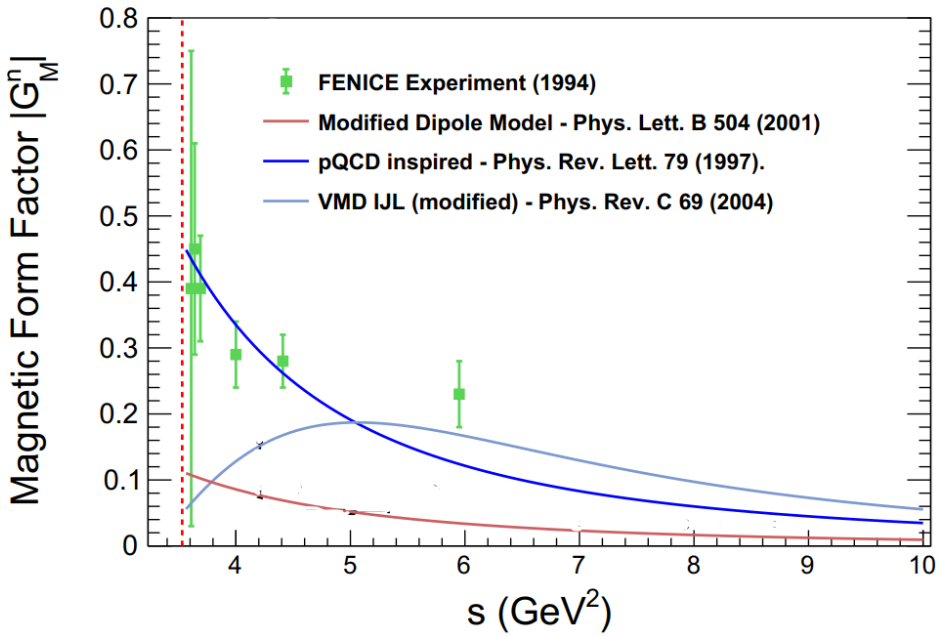

- Comparison of Magnetic Form Factor to the Theoretical Prediction:
  - The only existing results of $|G_M^n|$ are from Fenice, they were determined under the hypothesis $|G_E^n|=0$
  - **A comparison of $|G_M^n|$ results from this analysis to the various theoretical predictions is performed**

Status on hyperon FFs

- Rare experimental results on Hyperon FF

Phys. Rev. D **76,** 092006 (2007)

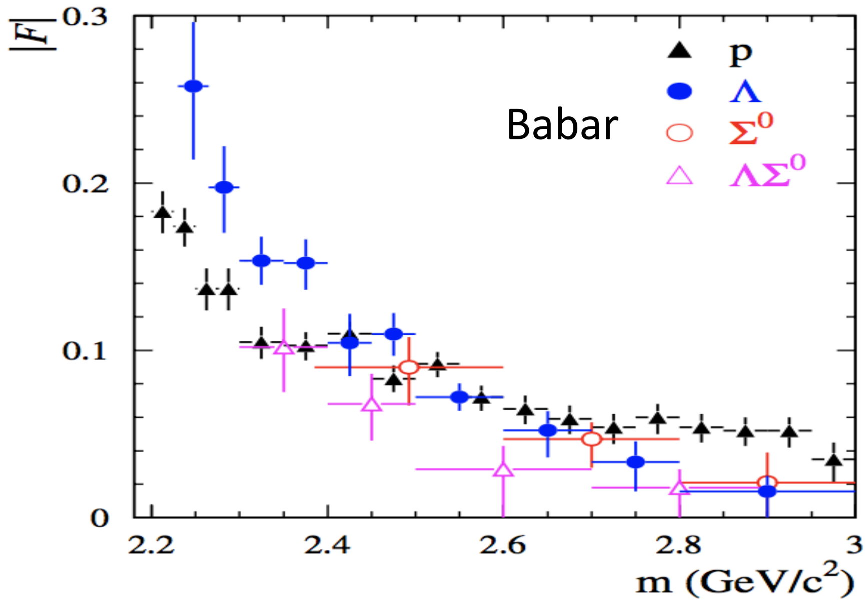

Phys. Lett. B 739 (2014) 90–94

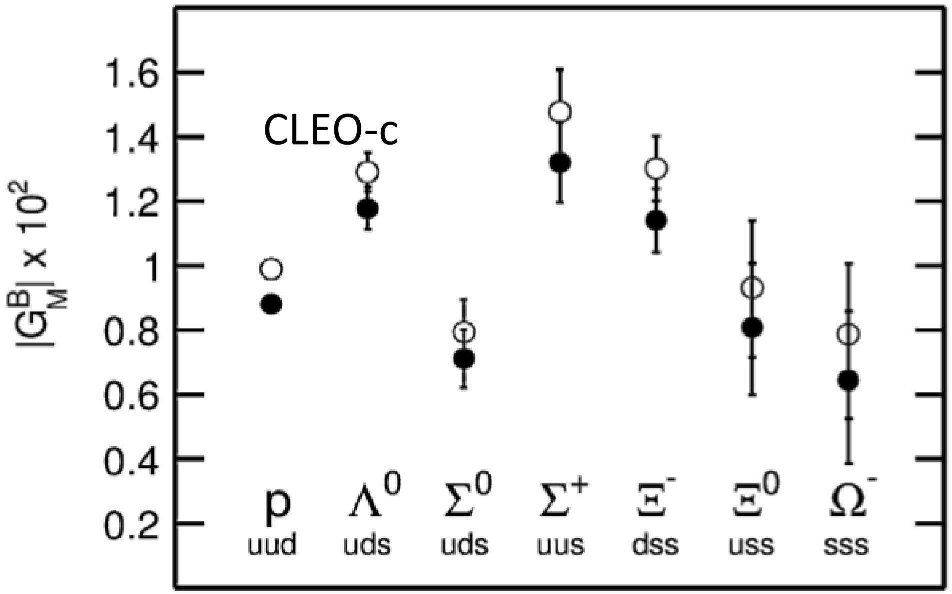

q^2=14.2 GeV^2

- diquark correlation evidence
- favor spin–isospin singlet

Measurement of Hyperon FFs near threshold

- The Born cross section for $e^+e^- \to \gamma^* \to B\bar{B}$, can be expressed in terms of electromagnetic form factor G_E and G_M :
  - $\sigma_{B\bar{B}}(q) = \frac{4\pi\alpha^2 C\beta}{3q^2}\left[|G_M(q)|^2 + \frac{1}{2\tau}|G_E(q)|^2\right]$
- The Coulomb factor $C=\frac{\pi\alpha}{\beta}\frac{1}{1-\exp(-\frac{\pi\alpha}{\beta})}$ for a charged $B\bar{B}$ pair, and equals to 1 for a neutral $B\bar{B}$ pair
- Complex form of FFs: $G_E = |G_E|e^{i\Phi_E}$, $G_M = |G_M|e^{i\Phi_M}$; Relative phase: $\Delta\Phi = \Phi_E$-Φ_M

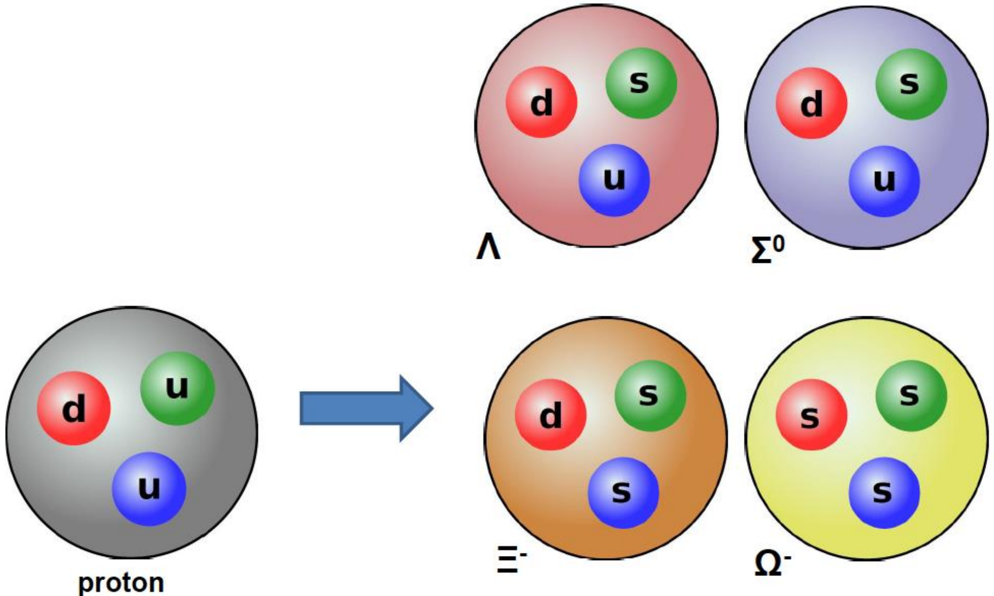

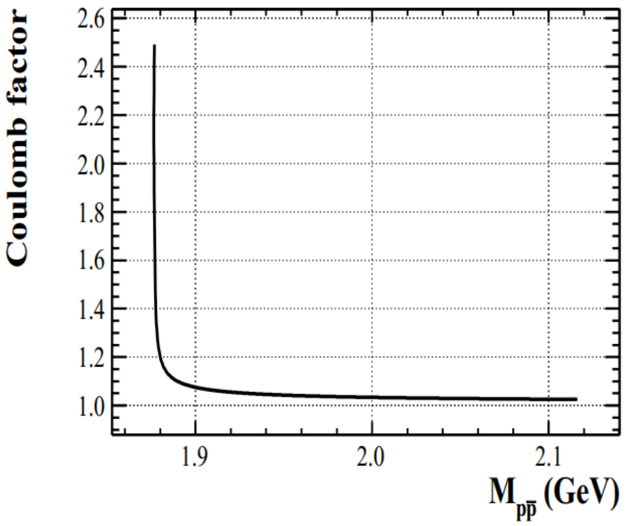

Determination of the Relative phase of FFs

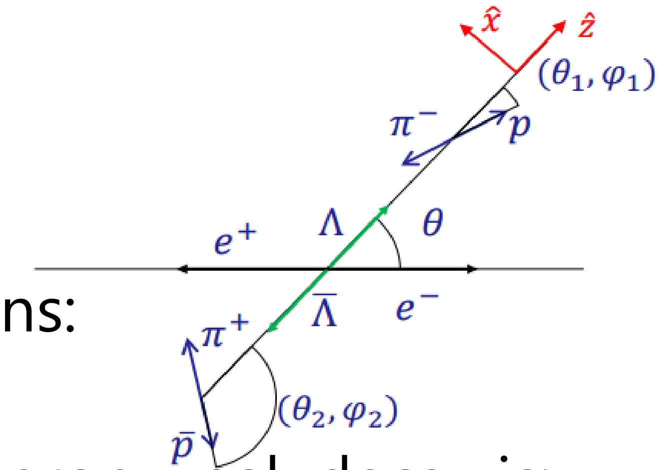

- Complex form of FFs:
  - $G_E = |G_E|e^{i\Phi_E}$, $G_M = |G_M|e^{i\Phi_M}$
  - Relative phase: $\Delta\Phi = \Phi_E$-Φ_M
- A non-zero phase has polarization effect on the Baryons:
  - $P_y \propto \sin \Delta\Phi$
- The angular distribution of daughter baryon from Hyperon weak decay is:
  - $\frac{d\sigma}{d\Omega} \propto 1 + \alpha_\Lambda \boldsymbol{P_y} \cdot \boldsymbol{\hat{q}}$
  - α_Λ: asymmetry parameter
  - $\hat{q}$: unit vector along the daughter baryon in hyperon rest frame

With hyperon weak decay to B+P, the polarization of hyperon can be measurement, so does the relative phase between G_E and G_M !

Complete measurement of Λ EMFFs

arXIv: 1903.09421

- An event of the reaction $e^+e^- \to \Lambda(\to p\pi^-)\overline{\Lambda}(\to \bar{p}\pi^+)$ is specified by the five dimensional vector $\xi = (\theta, \Omega_1, \Omega_2)$, the differential cross section is:

$$\begin{aligned}\mathscr{W}(\xi) = & \mathscr{T}_0(\xi) + \eta\,\mathscr{T}_5(\xi) \\ & -\alpha_\Lambda^2\left(\mathscr{T}_1(\xi) + \sqrt{1-\eta^2}\cos(\Delta\Phi)\,\mathscr{T}_2(\xi) + \eta\,\mathscr{T}_6(\xi)\right) \\ & +\alpha_\Lambda\sqrt{1-\eta^2}\sin(\Delta\Phi)\left(\mathscr{T}_3(\xi) - \mathscr{T}_4(\xi)\right).\end{aligned}$$

Phys.Lett. B772 (2017) 16-20

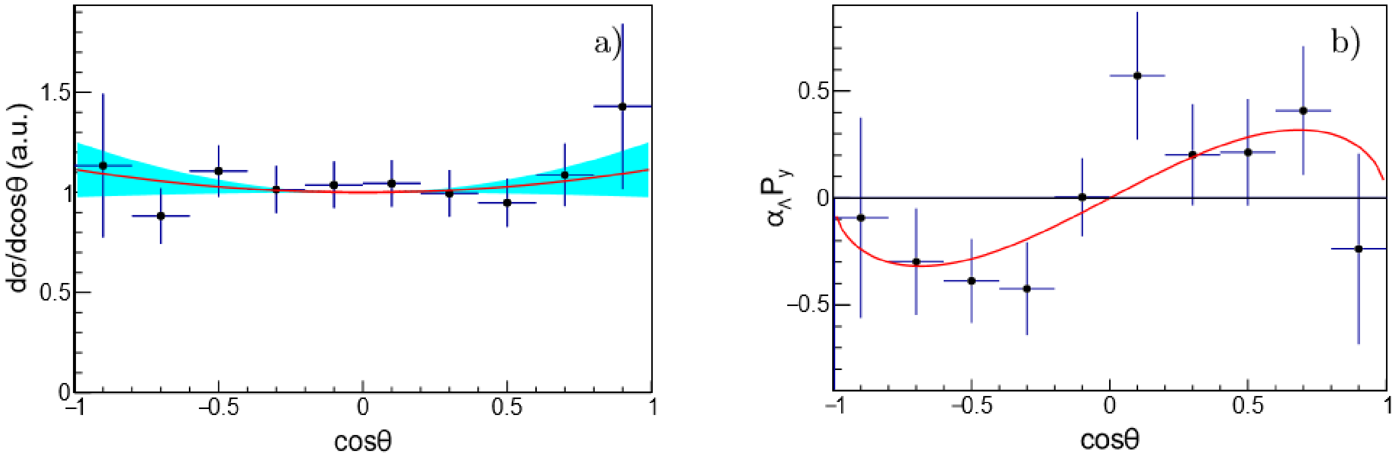

$$\left|\frac{G_E}{G_M}\right| = 0.96 \pm 0.14(stat.) \pm 0.02(sys.)$$

$$\Delta\Phi = 37^\circ \pm 12^\circ(stat.) \pm 6^\circ(sys.)$$

Fit data by Maximum Log Likelihood

Measurement of $e^+e^- \to \Lambda\bar{\Lambda}$ at $\sqrt{s}$ =2.2324 GeV

Phys. Rev. D 97, 032013 (2018)

- Near threshold production ($2M_\Lambda$ +1.0 MeV) and small PHSP in $\Lambda/\bar{\Lambda}$ decays
- Indirect search for antiproton in $\boldsymbol{\Lambda \to p\pi^-, \bar{\Lambda} \to \bar{p}\pi^+}$
- Search for mono-energetic π^0 in $\boldsymbol{\bar{\Lambda} \to \bar{n}\pi^0}$

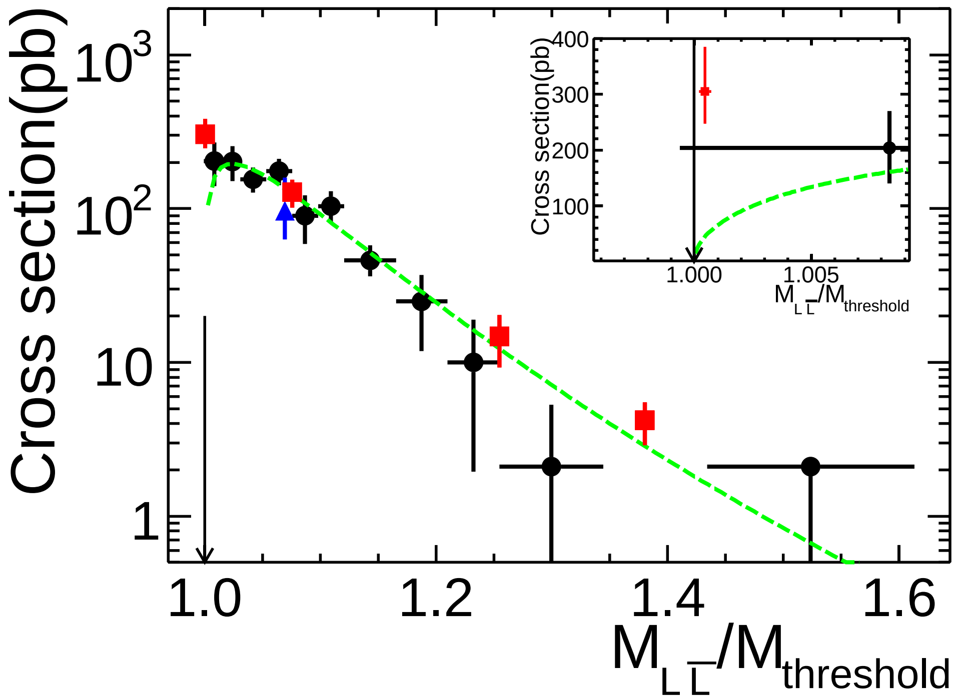

- The anomalous behavior differing from the pQCD prediction at threshold is observed.

•Recalling the baryon pair production cross section:

$\sigma_{B\bar{B}}(q) = \frac{4\pi\alpha^2 C\beta}{3q^2}[|G_M(q)|^2 + \frac{1}{2\tau}|G_E(q)|^2]$

•The Columb correction factor C=$\frac{\pi\alpha}{\beta}\frac{1}{1-\exp(-\frac{\pi\alpha}{\beta})}$(Q), cancel the β for a charged $B\bar{B}$ pair, equals to 1 for a neutral $B\bar{B}$ pair

A possible resonance around $\Lambda\bar{\Lambda}$ resonance?

Phys. Rev. D 100, 032009

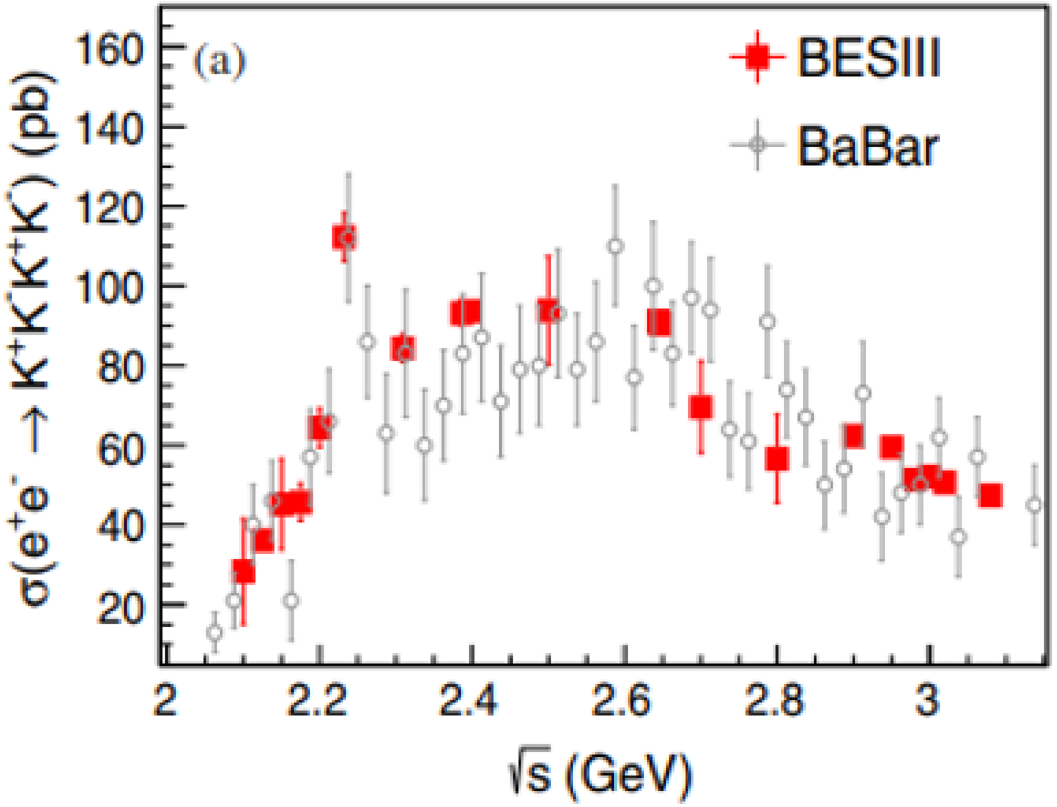

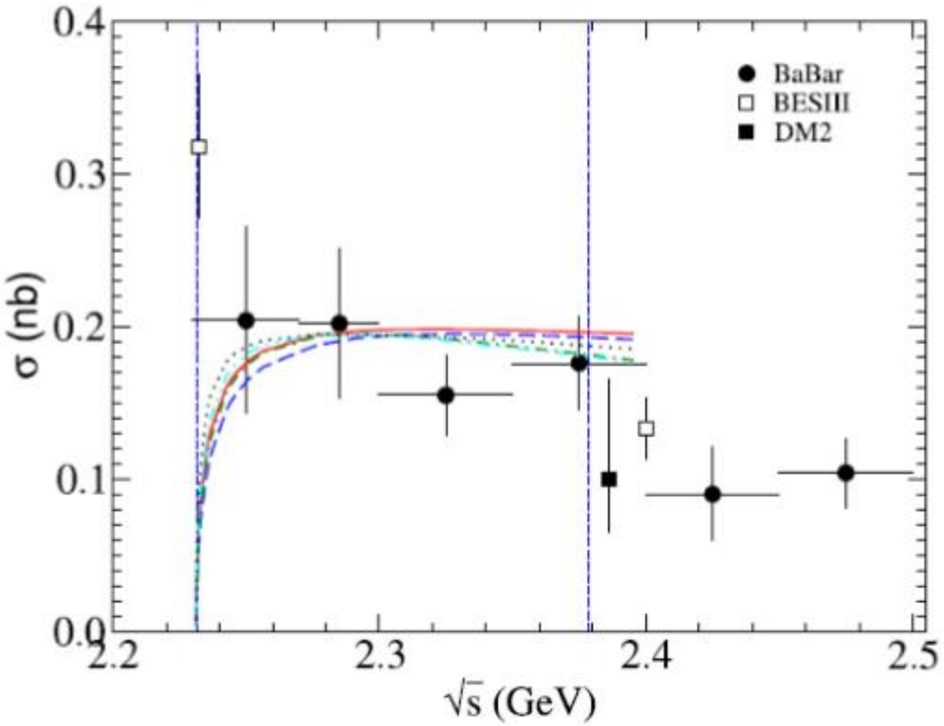

- A hint for resonance around $\Lambda\Lambda$ threshold in $e^+e^- \to KKKK$ cross section
  - Mass=2232±3.5 MeV， width≈20 MeV

$e^+e^- \to \Lambda_c^+\bar{\Lambda}_c^-$ near kinematic threshold

Phys. Rev. Lett. 120, 132001 (2018)

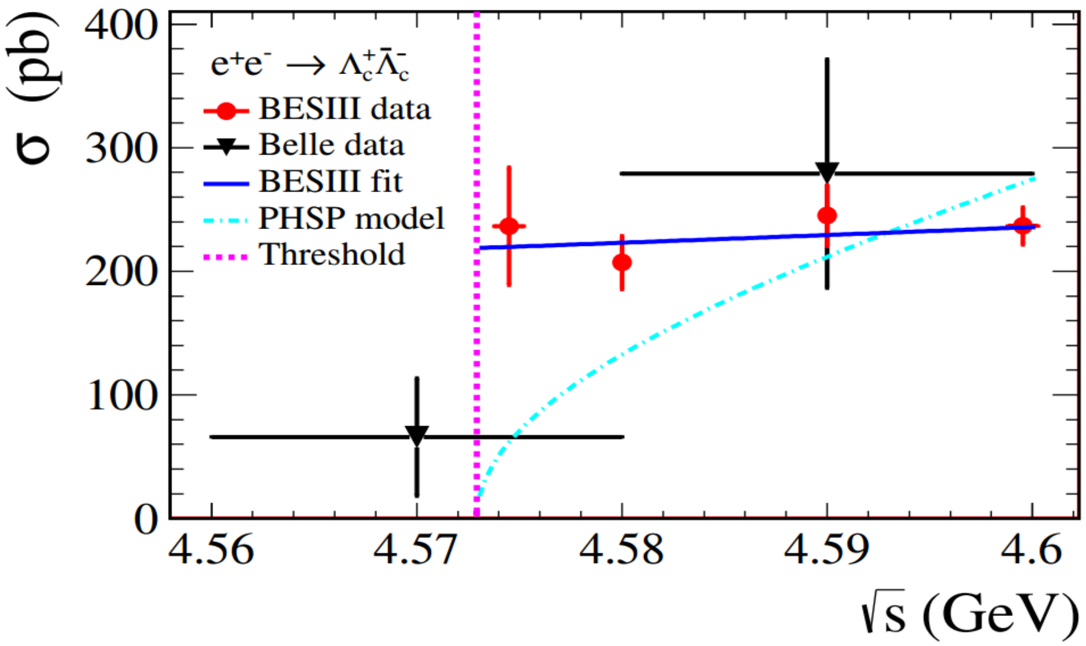

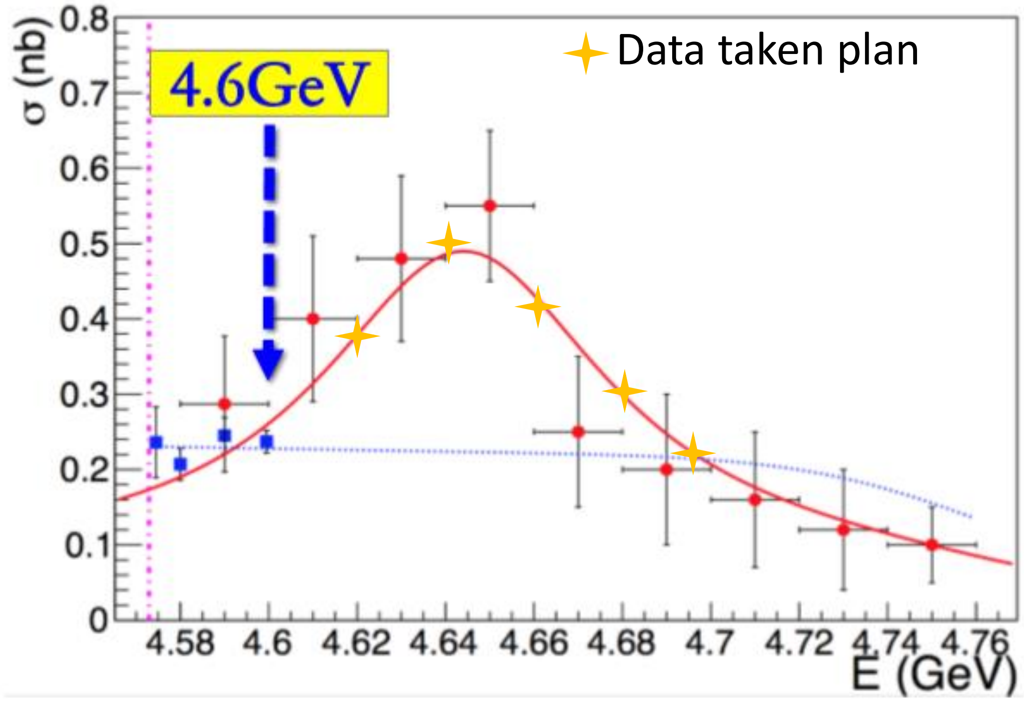

- Ten modes of Λ_c^+ ($\bar{\Lambda}_c^-$) are reconstructed
- Measurement of the Born cross section at 4 energy points below 4.6 GeV with **unprecedented statistical accuracy** (~1.3% at 4.6 GeV)

$e^+e^- \to \Lambda_c^+\bar{\Lambda}_c^-$ near kinematic threshold

- Angular distribution study

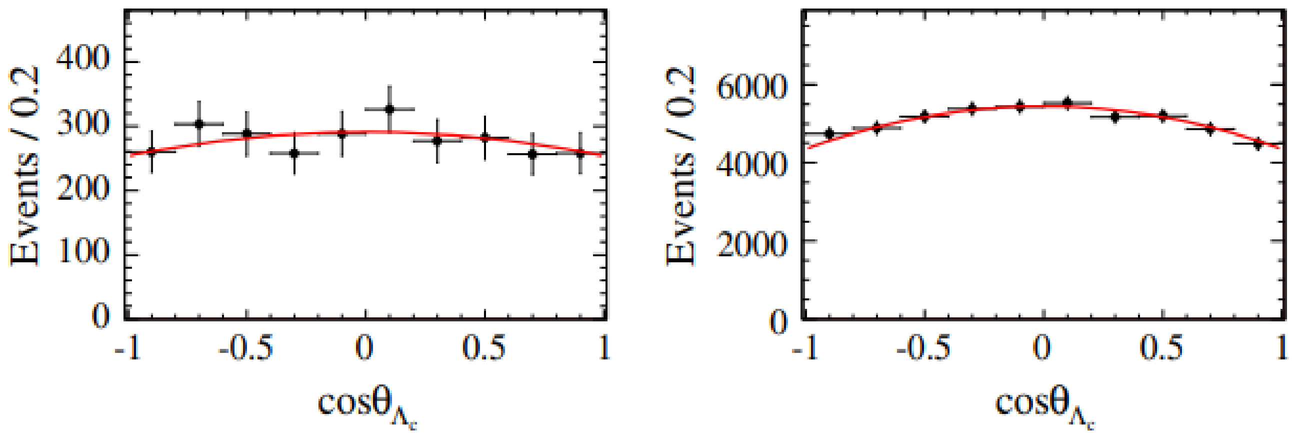

$\sqrt{s}$ (MeV)	α_{Λ_c}	$\lvert G_E/G_M \rvert$
4574.5	$-0.13 \pm 0.12 \pm 0.08$	$1.14 \pm 0.14 \pm 0.07$
4599.5	$-0.20 \pm 0.04 \pm 0.02$	$1.23 \pm 0.05 \pm 0.03$

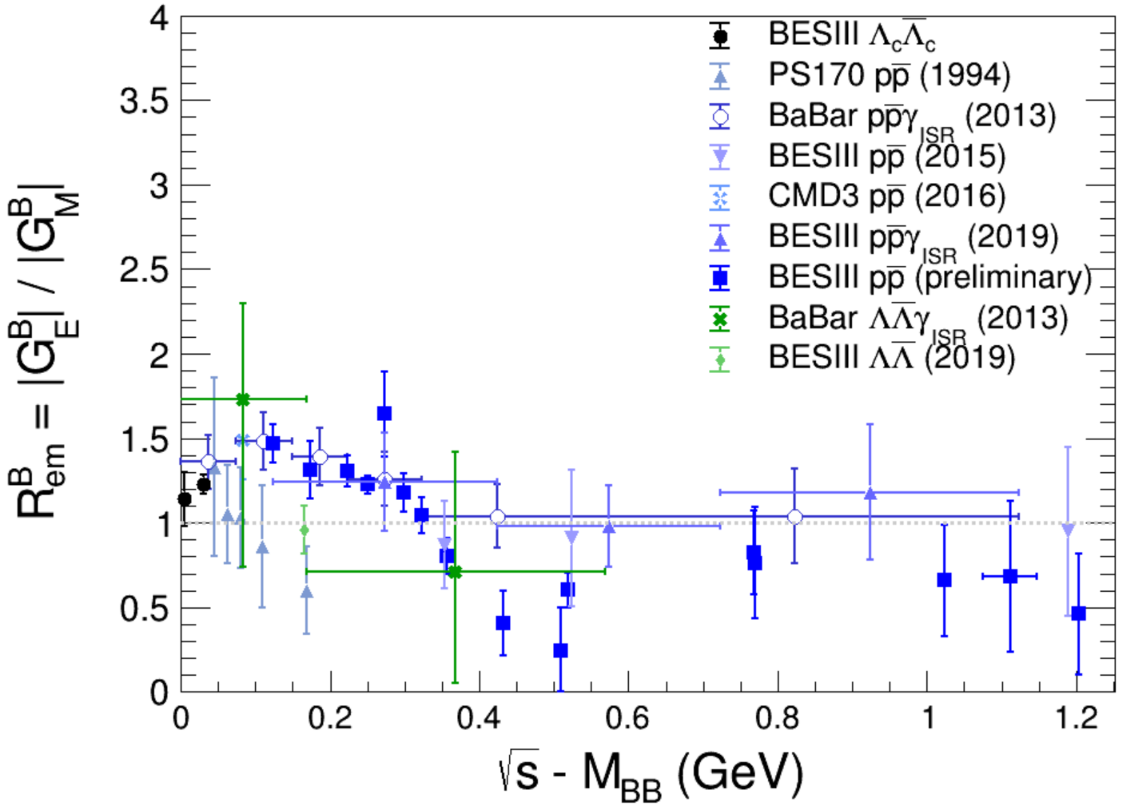

A summary of $|R_{EM}|$ for measured Baryons

Summary and discussion

- Nucleon FFs is measured with scan and ISR techniques at BESIII
  - Answered the remaining questions on proton FFs
  - Precise measurement on neutron FFs is ongoing
- With the large data set, more precise results on Hyperon FFs are expected on BESIII.
  - More precise cross section line-shape
  - Search for resonant structure and test di-quark correlation
  - Test on threshold effect
  - Complete determination of G_E and G_M

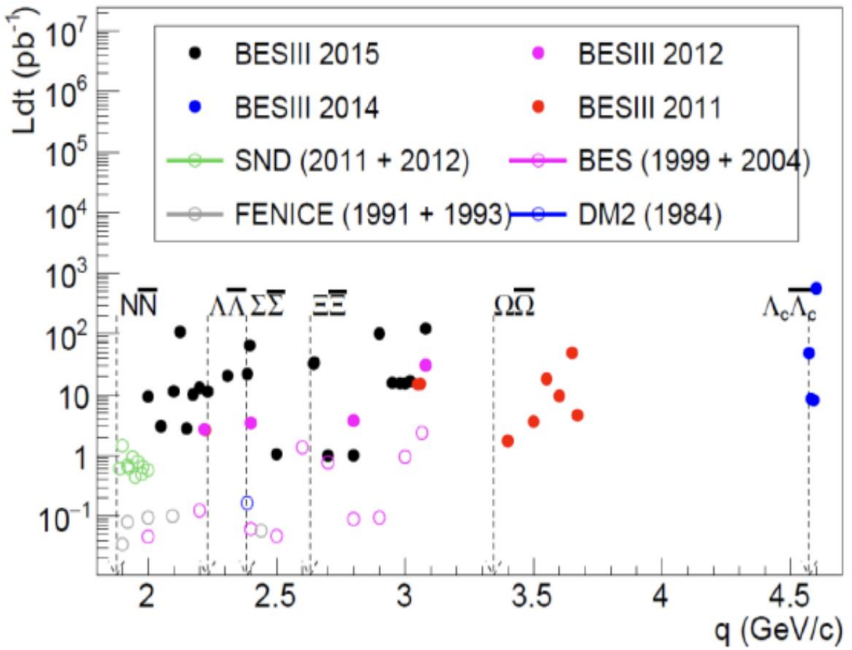

Energy scan in 2014-2015 at BESIII

Thank you for your attention!

Beijing Electron Positron Collider (BEPCII)

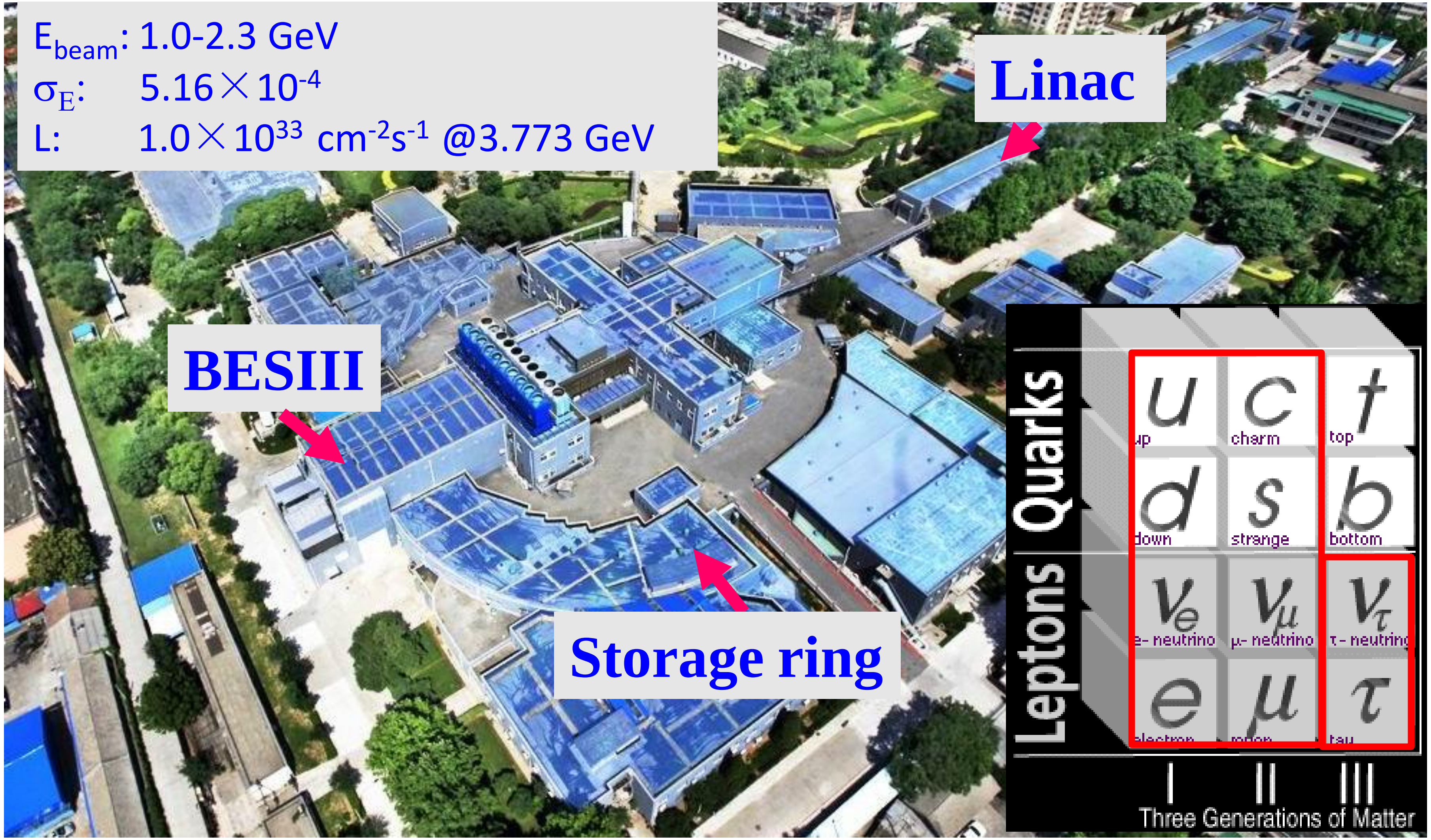

BESIII detector

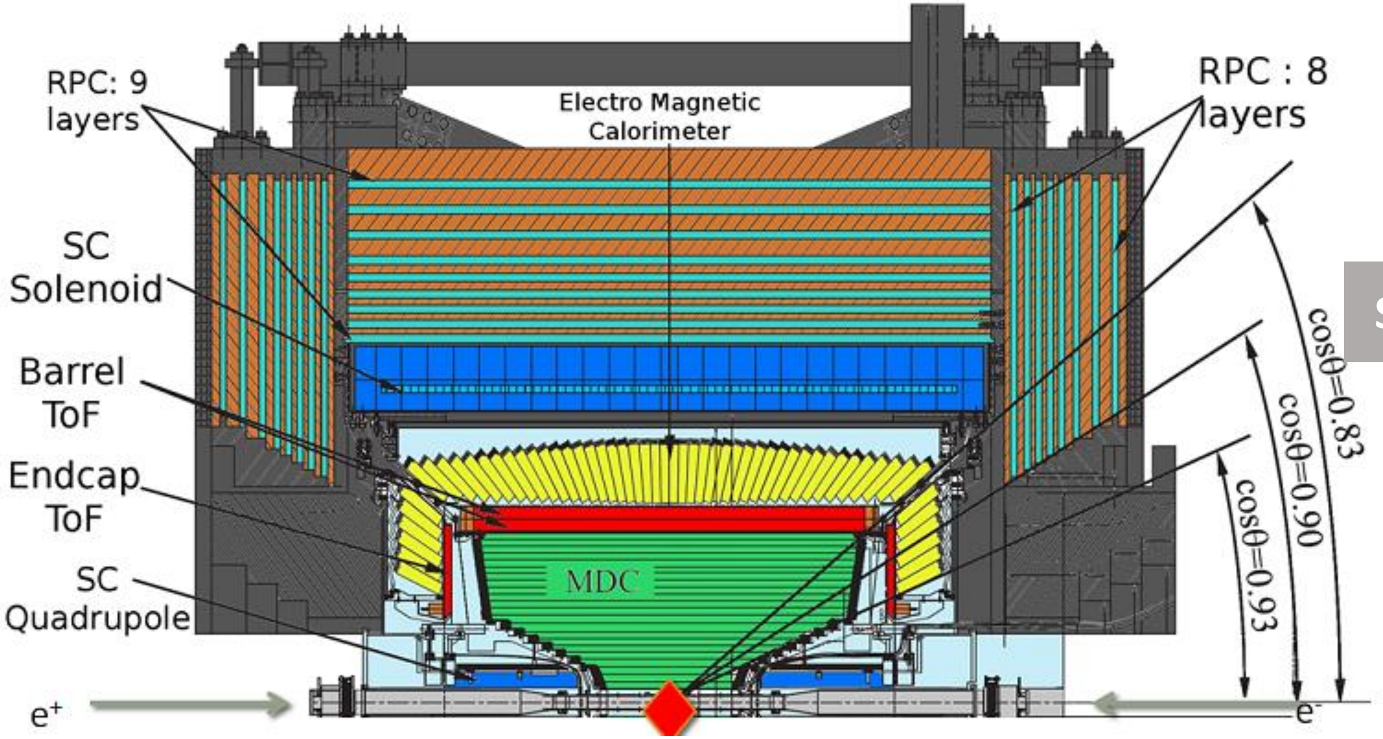

SC Magnet 1.0T

Main Drift Chamber
Small cell, 43 layer
σ_{xy}=130 μm, dE/dx~6%
σ_p/p = 0.5% at 1 GeV

Time Of Flight
Plastic scintillator
σ_T(barrel): 80 ps
σ_T(endcap): 110 ps
(endcap update with MRPC σ_T:65 ps)

Electromagnetic Calorimeter
CsI(Tl): L=28 cm ($15X_0$)
Energy range: 0.02-2GeV
Barrel σ_E 2.5%, σ_l 6mm
Endcap σ_E 5.0%, σ_l 9mm

Muon Counter
Resistive plate chamber
Barrel: 9 layers
Endcaps: 8 layers
$\sigma_{spatial}$: 1.48 cm